LETTER

Large magnetocaloric effect and critical behaviour analysis in Gd_2Cu_2In

To cite this article: K. Ramesh Kumar *et al* 2018 *EPL* **122** 17003

A Letters Journal Exploring the Frontiers of Physics

April 2018

EPL, **122** (2018) 17003 www.epljournal.org
doi: 10.1209/0295-5075/122/17003

Large magnetocaloric effect and critical behaviour analysis in Gd_2Cu_2In

K. Ramesh Kumar[1,2(a)], Harikrishnan S. Nair[3(a)], B. N. Sahu[1], Sindiwise Xhakaza[1] and André M. Strydom[1,4]

[1] *Highly Correlated Matter Research Group, Department of Physics, University of Johannesburg P. O. Box 524, Auckland Park 2006, South Africa*
[2] *Department of Condensed Matter Physics and Material Sciences, Tata Institute of Fundamental Research Colaba, Mumbai-400 005, India*
[3] *Department of Physics, University of Texas at El Paso - 500 W University Ave, El Paso, TX 79968, USA*
[4] *Max Planck Institute for Chemical Physics of Solids (MPICPfS) - Nöthnitzer Straße 40, 01187 Dresden, Germany*

received 5 February 2018; accepted in final form 9 May 2018
published online 29 May 2018

PACS 75.30.Sg – Magnetocaloric effect, magnetic cooling
PACS 75.40.Cx – Static properties (order parameter, static susceptibility, heat capacities, critical exponents, etc.)
PACS 75.30.Cr – Saturation moments and magnetic susceptibilities

Abstract – The ternary intermetallic compound Gd_2Cu_2In crystallizes in the Mo_2Fe_2B-type structure with the space group $P4/mbm$. The compound undergoes a ferromagnetic-paramagnetic (FM-PM) phase transition at 94.1 K and large magnetocaloric effect has been observed over a wide range of temperature. The isothermal magnetic entropy change (ΔS_m) and adiabatic temperature change (ΔT_{ad}) were observed to be 13.8 J/kg · K and 6.5 K for 7 T applied field. We have employed a modified Arrott plot (MAP) and Kouvel-Fisher (KF) procedures to estimate the critical exponents near the FM-PM phase transition. Critical exponents $\beta = 0.312(2)$ and $\gamma = 1.080(5)$ are estimated through a non-linear fitting. The β value is close to the three-dimensional (3D) Ising value, whereas γ and δ values lie closer to the mean-field values. Scaled magnetic isotherms collapse into two branches below and above T_C in accordance with a single scaling equation. Specific-heat measurements show a λ-type peak near 94 K indicating long-range magnetic ordering. The specific-heat exponent α was estimated by a non-linear fitting using the function $C_P = B + C\epsilon + A^{\pm}|\epsilon|^{-\alpha}(1 + E^{\pm}|\epsilon|^{0.5})$. The fitting in the temperature range $-0.025 < \epsilon < 0.025$ yields $\alpha = 0.11(3)$.

Introduction. – Magnetic materials with large magnetocaloric effect have attracted considerable attention due to their potential applications in magneto-refrigerant and eco-friendly cooling industries [1–3]. Among many possible compounds, RTX (R = rare earth; T = transition metal; X = p block element), RCo_2 (R = Er, Dy and Ho) based alloys [4], $Gd_5Si_2Ge_2$ and related compounds [5], Ni-Mn-X based Heusler alloys, $RMnO_3$ (R = lanthanide) manganites [6], MnAs compounds [2], and $LaFe_{13-x}Si_x$ based intermetallic compounds [7] have drawn much attention due to giant magnetocaloric effect and large relative cooling power (RCP). The compounds R_2Cu_2In crystallize in a tetragonal structure with the space group $P4/mbm$ and the structure can be derived from the U_3Si_2-type structure. The R and indium atoms occupy the U sites, whereas transition metal atoms occupy the Si site [8,9]. Fisher *et al.* have synthesized the single crystalline Gd_2Cu_2In and observed ferromagnetic ordering below 85 K with tetragonal "c" as easy axis [8]. Recently, several researchers studied the structural, magnetic and magneto-thermal properties of R_2Cu_2X (R = Er, Tm, Ho and Dy; X = Cd, In) due to the presence of large magnetocaloric effect [10–15]. For instance, the compound Dy_2Cu_2In crystallizes in the Mo_2Fe_2B tetragonal structure and exhibits two successive magnetic transitions at 49.5 K and 19.5 K. The compound showed large magnetocaloric effect (16.5 J/kg · K) with a RCP value 617 J/kg [13] at 7 T. Similarly, the systems

[(a)] These authors contributed equally to this paper.

$Ho_2(Cu,Au)_2In$ showed antiferromagnetic ordering below 30 K and possess magnetic entropy change 21.9 J/kg · K (Cu) and 15.8 J/kg K (Au) for 7 T applied field [14]. Critical exponent analysis is an effective tool for understanding the magnetic phase transitions and to study the intrinsic nature of the ferromagnetism in alloys, amorphous materials and rare-earth manganites [16–19]. In this manuscript we report on the magneto-thermal analysis and magnetocaloric effect in Gd_2Cu_2In. Critical behaviour and scaling analysis are carried out by employing the modified Arrott plot, Kouvel-Fisher technique and critical scaling methods.

Experimental details. – A polycrystalline sample was synthesized by arc-melting the stoichiometric mixture of high-purity (99.9 wt% or better) elements under argon atmosphere. The arc-melted sample was wrapped using a tantalum foil and placed in an evacuated quartz ampule. The sample was heat-treated at 800 °C for 7 days and then subsequently quenched in the iced water. Crystal structure analysis was done using powder x-ray diffraction and Rietveld refinement [20,21]. Magnetic measurements were carried out using the commercial superconducting quantum interference device based magnetometer (Quantum Design Inc., San Diego) in the temperature range between 1.8 and 300 K. Magnetization isotherms were collected with a 5 K temperature interval above and below T_C and near the transition we collected M-H data with 2 K interval. In order to avoid the field cycling effects, the M-H isotherms were recorded by heating the sample till 150 K for every cycle of measurement. Specific-heat (C_P) measurements were carried out in the temperature between 2 and 300 K using the physical property measurement system (Quantum Design Inc., San Diego).

Results and discussion. –

Crystal structure details. Figure 1(a) shows the indexed x-ray diffraction pattern along with the Rietveld refinement fit. The XRD pattern could be indexed by Bragg's reflections which are allowed within the $P4/mbm$ space group. The analysis confirms the single-phase nature of the sample. The estimated lattice parameter values are $a = b = 7.5231(9)$ Å and $c = 3.8099(5)$ Å and the values are in agreement with the previously reported lattice parameter values [22]. Figure 1(b) depicts the crystal structure of Gd_2Cu_2In projected along the c-axis. In this structure, the Gd and Cu respectively occupy $4h$ and $4g$ Wyckoff positions, whereas In occupies the $2a$ site. The structure can be viewed as stacking of two alternating layers with one layer containing Gd atoms exclusively and the other layer containing Cu and In atoms. There are two different nearest neighbours among Gd atoms with $d_{Gd\text{-}Gd1} = 3.6229(5)$ Å and $d_{Gd\text{-}Gd2} = 3.8099(5)$ Å and in the basal plane there is an additional nearest neighbour with $d_{Gd\text{-}Gd3} = 3.9480(5)$ Å. The coordination shell of a Gd atom is surrounded by 6 Cu, 4 In and 3 Gd atoms. The Gd-Cu interatomic distances range from 2.9048(3) Å to 2.9650(3) Å which is significantly larger than the sum of the metallic radii for CN 12 of 3.08 Å.

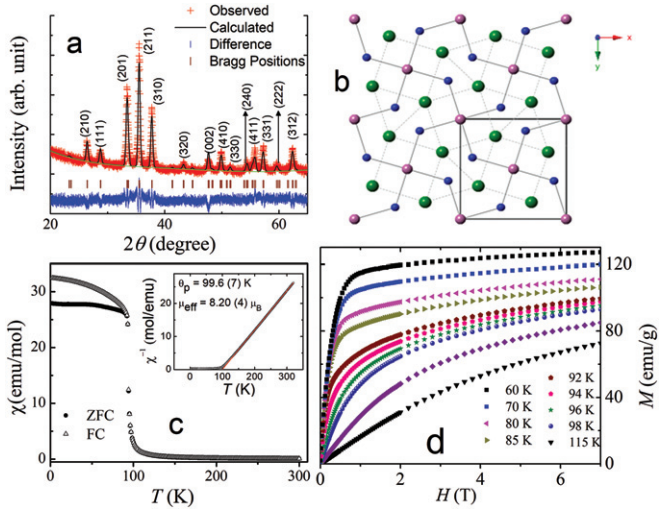

Fig. 1: (Colour online) (a)–(d) (a) Rietveld refinement of a powder X-ray diffraction pattern using the $P4/mbm$ space group. (b) The crystal structure of Gd_2Cu_2In is projected along the c-axis. The Gd atoms are represented by green circles, whereas Cu and In atoms are represented by pink and blue circles, respectively. (c) Temperature variation of the magnetic susceptibility (FC-ZFC) under the field value of 10 mT. The inset shows the temperature variation of the inverse susceptibility along with Curie-Weiss fitting (red solid line). (d) Isothermal magnetization data for selected temperatures close to T_C.

Magnetic properties. Figure 1(c) presents the temperature variation of the magnetic susceptibility in the ZFC and FC protocol for 10 mT applied field. The magnetic susceptibility showed typical temperature behaviour for a ferromagnetic materials and the Curie temperature is observed to be 94.1 K. Below T_C the susceptibility showed a divergent behaviour between FC and ZFC measurements which may indicate the presence of a uniaxial magnetic anisotropy and short-range magnetic ordering. The inset of fig. 1(c) shows the temperature variation of the inverse susceptibility along with Curie-Weiss linear fit. From the analysis, the effective magnetic moment (μ_{eff}) and the Curie-Weiss temperature (θ_P) are estimated to be 8.20(4) μ_B and 99.6(7) K, respectively. The estimated effective moment is larger than the free-ion value expected for a Gd^{3+} ion ($g\sqrt{J(J+1)} = 7.94\mu_B$). This excess effective moment could be attributed to the formation of a polarization cloud of the conduction electron. By assuming a local Gd moment and ${\mu_{eff}}^2 = {\mu_{Cu}}^2 + {\mu_{Gd}}^2$, the excess magnetic moment can be estimated as $1.9\mu_B$ which is close to the spin-only moment of a Cu^{2+} ion. Figure 1(d) shows a set of magnetic isotherms collected in the temperature range between 60 and 120 K with 5 K intervals. The field dependence of magnetization showed a typical sigmoid behaviour expected for ferromagnetic materials. The saturation magnetization at 2 K was observed to be 7.13μ_B

and the value is slightly larger than the expected value for trivalent Gd ($gJ = 7\mu_B$).

Magnetocaloric properties. In the literature, the magnetocaloric effect is characterized by the isothermal magnetic entropy change ΔS_m and the adiabatic temperature change ΔS_m in the presence of an external magnetic field. ΔS_m can be estimated by the following Maxwell relation [1,2]:

$$\Delta S_m(T,H) = \int_{H_i}^{H_f} \left(\frac{\delta M}{\delta T}\right)_H \mathrm{d}H'. \tag{1}$$

The temperature variation of the magnetic entropy change ($-\Delta S_m$) shows positive values with single-peak behaviour (fig. 2(a)). The maximum entropy change for the 7 T field was 13.8 J/kg · K and even for 5 T the system exhibits a large ΔS_m value of 11.4 J/kg · K. Among R_2Cu_2X (R = Tm, Er, Dy, Ho and Gd; X = In and Cd) compounds, Dy, Ho and Er based systems showed larger MCE compared to Gd based sample due to multiple transitions (see table 1). The field dependence of the magnetic entropy change follows a power law relation

$$(\Delta S_m^{pk})_{T=Tc} = H^n, \tag{2}$$

where n is the local exponent [23]. With mean-field approximation, the "n" value is estimated to be 0.66 and for other models the local exponent shows a significant deviation from 2/3. The local exponent (n) can be estimated by fitting the $\ln(\Delta S_m^{pk})_{T=Tc}$ *vs.* $\ln H$ data and from the fitting we observed the "n" value to be 0.60(2). The deviation from 2/3 may indicate that the system belongs to a different universality class (fig. 2(c)).

The adiabatic temperature change (ΔT_{ad}) is estimated using the following relation [2];

$$\Delta T_{ad}(T,H) = -\frac{T\Delta S_M}{C_P(T,H)}. \tag{3}$$

The temperature variation of ΔT_{ad} resembles the temperature variation of ΔS_m till 3 T field. However, we observed the ΔT_{ad} deviates from a smooth peak function for the higher field (fig. 2(b)). Our estimate gives a lower bound value of ΔT_{ad} which is an important parameter and not estimated in the iso-structural compounds [10,12,14].

Recently, Franco *et al.* have proposed a universal scaling for the magnetocaloric effect to distinguish the first- and the second-order phase transitions [24]. According to this model, the normalized entropy change $\Delta S_M/\Delta S_M^{max}$ (where ΔS_M^{max} is the maximum entropy change) against scaled temperature (θ) merges into a single curve for any second-order phase transition and disperses into branches in the case of a first-order transition [24,25]. Universal scaling is done by rescaling the temperature axis with two reference temperatures *viz.* T_{r1} and T_{r2},

$$\theta = \begin{cases} -(T-T_C)/(T_{r1}-T_C), & T < T_C, \\ (T-T_C)/(T_{r2}-T_C), & T > T_C. \end{cases} \tag{4}$$

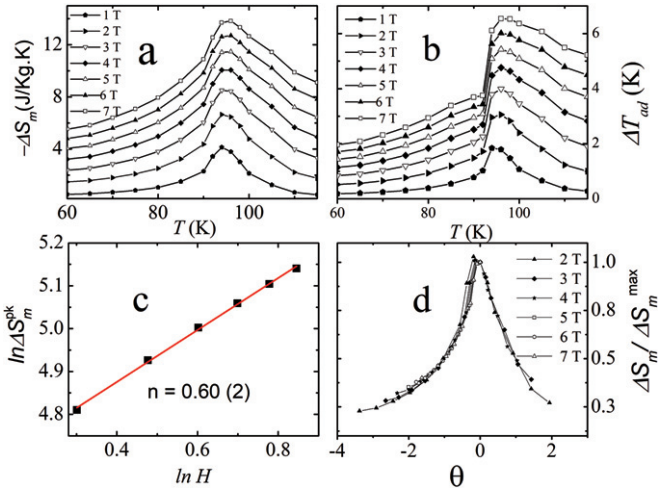

Fig. 2: (Colour online) Temperature variation of the magnetic entropy change $-\Delta S_m$ (a) and adiabatic temperature ΔT_{ad} (b) estimated using Maxwell's relations. (c) $\ln(\Delta S_m^{pk})_{T=Tc}$ *vs.* $\ln H$ plot along with the linear fit (solid red line). (d) Normalized entropy change ($\Delta S_M/\Delta S_M^{max}$) as a function of the scaled temperature (θ) for a selected applied field.

The reference temperatures are chosen for each field in such a way that

$$\Delta S_m(T_{r1})/\Delta S_m^{max} = \Delta S_M(T_{r2})/\Delta S_m^{max} = h \quad (0 < h < 1). \tag{5}$$

Figure 2(d) shows the normalized entropy change with respect to the scaled temperature constructed by assuming $h = 0.5$. The normalized entropy collapsed into a single curve for the entire temperature range as expected for a second-order phase transition (see fig. 2(d)).

The relative cooling power (RCP) is defined as the amount of heat transfer between the hot and the cold reservoirs in an ideal refrigeration cycle. The RCP is mathematically expressed as follows:

$$RCP = \Delta S_m^{max} \times \delta T_{FWHM}, \tag{6}$$

where δT_{FWHM} is the full width at half-maximum of ΔS_M *vs.* T curve. In the present investigation, the RCP values for the 0–5 T and 0–7 T applied field were 225 J/kg and 360 J/kg, respectively (see table 1).

Critical behaviour and scaling analysis. Figure 3(a) shows the conventional Arrott plot for the compound Gd_2Cu_2In constructed by plotting $\mu_0 H/M$ against M^2. The Arrott plot assumes mean-field behaviour with $\beta = 0.5$ and $\gamma = 1$. For the right choice of the critical exponents, it is expected that the high-field magnetization should show a set of parallel lines near T_C. Further, the critical isotherm at $T = T_C$ should pass through the origin. From fig. 3(a) it is clear that the magnetic isotherms show a quasi-linear behaviour and the critical isotherm does not pass through the origin. Hence, mean-field exponents might not be suitable to describe the phase transition in Gd_2Cu_2In. We employed a modified Arrott plot

Table 1: Ordering temperature, magnetic entropy change, adiabatic temperature change, relative cooling power for Gd_2Cu_2In are compared with some selected R_2Cu_2X compounds.

Compound	Transition K	ΔS_M^{max} (J/kg·K)	RCP (J/kg)
Dy_2Cu_2In [15]	49.5	13.3	409
Ho_2Cu_2In [14]	30	23.6	416
Ho_2Au_2In [14]	21	15.1	229
Dy_2Cu_2Cd [10]	48	13.8	381
Er_2Cu_2Cd [12]	36	15.4	336
Gd_2Cu_2Cd [12]	120	7.8	314
$Gd_2Cu_2In^*$	94	11.4	225

*Present study.

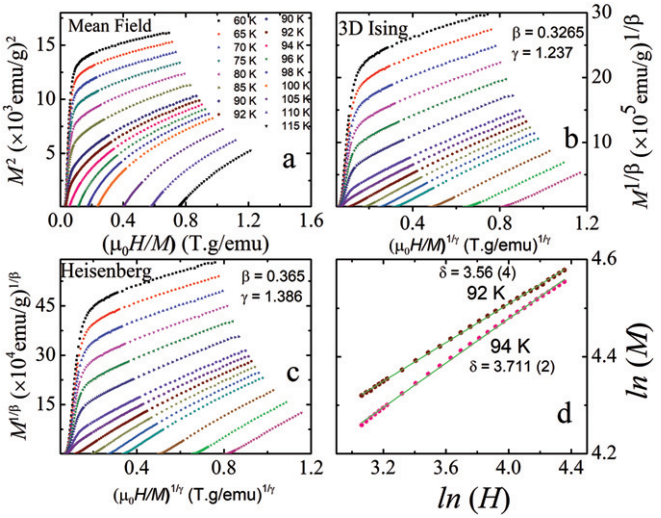

Fig. 3: (Colour online) (a) Conventional Arrott plot isotherms ($\mu_0 H/M$ *vs.* M^2) for selected temperatures. (b) and (c): modified Arrott plots ($(\mu_0 H/M)^{1/\gamma}$ *vs.* $M^{1/\beta}$) using the theoretical exponents corresponding to 3D Ising (b) and Heisenberg (c) models. (d) Critical isotherms are shown in logarithmic scale. The green line represents a linear fit.

technique to estimate the correct set of critical exponents. According to the Arrott-Noakes theorem, the magnetization (order parameter) can be written as

$$(\mu_0 H/M)^{1/\gamma} = a\left(\frac{T - T_C}{T}\right) + bM^{1/\beta}, \qquad (7)$$

where a and b are constants; β and γ are critical exponents. The spontaneous magnetization ($M_S(T)$), initial susceptibility ($\chi_0^{-1}(T)$) and critical isotherms are characterized by a set of three critical exponents *viz.* β, γ and δ, respectively. These exponents are strongly interrelated and depend only upon the lattice dimension (d) and spin dimensionality (n_s). The spontaneous magnetization and initial susceptibility can be expressed as power law equations [26],

$$M_s(T) = M_0(-\epsilon)^{\beta}, \quad \epsilon < 0, \quad T < T_C, \qquad (8)$$

$$\chi_0^{-1}(T) = (h_0/M_0)\epsilon^{\gamma}, \quad \epsilon > 0, \quad T > T_C, \qquad (9)$$

$$M = DH^{1/\delta}, \quad \epsilon = 0, \quad T = T_C, \qquad (10)$$

where $\epsilon = (T - T_C/T_C)$ is the reduced temperature; M_0, h_0, m_0 and D are known as critical amplitudes. Further, in the critical region, the magnetic equation of state can be written as follows:

$$M(H, \epsilon) = \epsilon^{\beta} f_{\pm}(H/\epsilon^{\beta+\gamma}), \qquad (11)$$

where f_- and f_+ are regular analytic functions corresponding to below and above T_C.

The magnetization (M) and the field (H) can be renormalized in such a way that the $m \equiv \epsilon^{-\beta} M(H, \epsilon)$ *vs.* $h \equiv \epsilon^{-\beta+\gamma} H$ plot collapses into two branches below and above T_C. Branching of renormalized magnetic isotherms validates the estimation of critical exponents and of the universality class. Initially, a modified Arrott plot is constructed using eq. (7) and a set of β and γ values. The spontaneous magnetization and initial susceptibility are estimated by linear extrapolation of high field data to $M^{1/\beta}$ and $(H/M)^{1/\gamma}$, respectively. The $M_S(T)$ *vs.* T and $\chi_0^{-1}(T)$ *vs.* T data are fitted with eqs. (8) and (9) to obtain a new set of β and γ values. This procedure is repeated until the critical exponents converge to stable values. We have followed a similar procedure to estimate β and γ, however, the initial values and the universality class are guessed in order to avoid many cycles of constructing MAPs. Figure 3(a)–(c) shows both conventional and modified Arrott plots for mean-field, 3D Ising and 3D Heisenberg models using the theoretical exponent values (see table 2). It is clear from the plots that the 3D Ising and 3D Heisenberg models may be suitable for this system as the high field data exhibiting a set of parallel lines (fig. 3(b) and (c)). In order to further narrow down the possible values, we have computed the relative slope $RS \equiv S(T)/S(T_C)$ for the full temperature range (where ($S(T)$ and ($S(T_C)$) are slopes of the magnetic isotherms corresponding to the temperatures T and $T = T_C$)). The relative slope value is expected to be 1 for the most suitable critical behaviour. In the present investigation the RS change for the 3D Ising exponents showed a 22% deviation, whereas the mean-field and 3D Heisenberg exponents show more than 30% deviation from the expected values. Hence, we believe that the system could be renormalized into the 3D Ising universal class. The local exponent "n" is related to the critical exponents through the following relation [27]:

$$n = 1 + \frac{\beta - 1}{\beta + \gamma}, \qquad (12)$$

using Widom's scaling ($\delta = 1 + \gamma/\beta$), expression (12) can be re-written as

$$n = 1 + \frac{1}{\delta}\left(1 - \frac{1}{\beta}\right). \qquad (13)$$

Table 2: The critical exponents (β, γ, δ and α) estimated from the modified Arrott plot technique (MAP), Kouvel-Fisher method (KF), critical isotherm (CI) and heat capacity exponent are compared with the theoretical critical exponents.

Technique	β	γ	δ	α	A^+/A^-
MAP	0.312(2)	1.080(5)			
KF	0.331(8)	1.034(6)			
CI			3.711(2)		
C_P				0.11(1)	0.49(2)
		Theory			
Mean field	0.5	1.0	3.0	0	–
3D Ising	0.325	1.24	4.8	0.11	0.524
Heisenberg	0.365	1.386	4.82	−0.115	1.521

Figure 3(d) shows the critical isotherms along with a linear fit for 92 K and 94 K. The δ values were estimated to be 3.56(4) and 3.711(2) for 92 K and 94 K, respectively. Using the n and δ values we derived the initial values of β and γ to construct the modified Arrott plots. Figure 4(a) shows the temperature variation of spontaneous magnetization and initial susceptibility along with the non-linear fit using the expressions (8) and (9). From the final fitting, the estimated values are $\beta = 0.312(2)$; $T_C = 92.97(4)$ $T < T_C$ and $\gamma = 1.08(5)$ $T_C = 93.3\,\mathrm{T} > T_C$. The β value is close to the 3D Ising value, whereas the γ value signifies a mean-field–type behaviour. According to the Kouvel-Fisher method, the power law behaviour of the magnetization (eq. (8)) and initial susceptibility (eq. (9)) can be deduced to a simple linear function by dividing the respective first-order derivatives. Hence, the functions $M_S(\mathrm{d}M_S/\mathrm{d}T)^{-1}$ and $\chi^{-1}(\mathrm{d}\chi^{-1}/\mathrm{d}T)^{-1}$ follow a linear relation against temperature with slope $1/\beta$ and $1/\gamma$. Figure 4(c) shows a $M_S(\mathrm{d}M_S/\mathrm{d}T)^{-1}$ and $\chi^{-1}(\mathrm{d}\chi^{-1}/\mathrm{d}T)^{-1}$ *vs.* T plot along with the linear fitting. The estimated exponents are $\beta = 0.331(8)$; $T_C = 93.33(5)$ $T < T_C$ and $\gamma = 1.034(6)$ $T_C = 93.54(1)$ $T > T_C$. According to the scaling hypothesis, the reliability of the obtained critical exponents can be verified by the universal scaling of the magnetization curves. Using the critical exponents observed from the KF method, we constructed $m \equiv \epsilon^{-\beta}M(H,\epsilon)$ *vs.* $h \equiv \epsilon^{-\beta+\gamma}H$ plot (see fig. 4(d)). It can be seen that all the isotherms collapse into two different branches below and above T_C. Branching of the magnetic isotherms indicates that the computed values are reliable and obey the universal scaling.

The fourth critical exponent α can be estimated from the heat capacity measurements. Since α can be estimated from the zero-field heat capacity, the uncertainty due to the demagnetization field/residual field presence in the magnetization measurements can be avoided. For antiferromagnetic systems, α is a useful parameter because magnetization need not be considered as the order parameter. Zero-field C_P data near the transition temperature is fitted to the following relation:

$$C_P = B + C\epsilon + A^{\pm}|\epsilon|^{-\alpha}(1 + E^{\pm}|\epsilon|^{0.5}) \qquad (14)$$

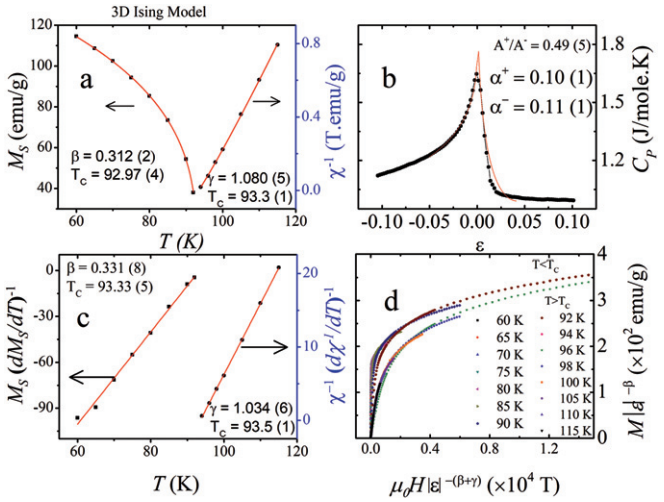

Fig. 4: (Colour online) (a) Temperature variation of spontaneous magnetization and initial susceptibility along with non-linear fit using the expressions (8) and (9). (b) Experimental (black circles) and fitted curves (red line) of the specific heat as a function of the reduced temperature in the vicinity of T_C using eq. (14). (c) Kouvel-Fisher plot for the spontaneous magnetization and initial susceptibility (solid red lines represent the linear fit). (d) Scaling plots of $M\epsilon^{-\beta}$ *vs.* $H\epsilon^{-(\beta+\gamma)}$ below and above T_C using the estimated critical exponents ($\beta = 0.331$ and $\gamma = 1.034$).

where ϵ is the reduced temperature; $A^{\pm}$, B, C and $E^{\pm}$ are adjustable parameters. The relevant information about the critical behaviour of the heat capacity and fitting procedures can be found in refs. [28,29]. Figure 4(b) shows the temperature variation of the heat capacity along with the non-linear fit using the expression (14). From the fitting the estimated values are $\alpha^+ = 0.10(1)$, $\alpha^- = 0.11(1)$ and $A^+/A^- = 0.49(5)$. The estimated critical exponents along with the theoretical values are summarized in table 2. The critical exponent (α) and the ratio value A^+/A^- point towards 3D Ising behaviour both below and above T_C as opposed to the magnetization studies where the estimation indicated a crossover behaviour from 3D Ising to mean-field behaviour across the transition. Crossover behaviour is often observed in many hole-doped $RMnO_3$ (R = Lanthanide) manganites. Kim *et al.* have observed in the $La_{0.75}Sr_{0.25}MnO_3$ sample that the critical exponents lie between 3D Ising model values and mean-field values [19]. Critical behaviour of $CrSiTe_3$ showed a 2D Ising-type critical behaviour coupled with long-range spin interactions [30]. Recently, Dey *et al.* have observed through magneto-thermal measurements that the system $MnCr_2O_4$ possesses critical exponents which lie between 3D Heisenberg and mean-field behaviour [31]. It is important to understand the crossover behaviour in terms of length and temperature scales. The correlation length $\xi = \xi_0|\epsilon|^{-\upsilon}$, where υ is the correlation length exponent, can be roughly estimated by using the relation $\upsilon = (2-\alpha)/d$ [19]; by assuming typical values for ξ_0 to

be 5–10 Å we estimated the correlation length to be 51 Å up to 102 Å for $\epsilon \approx 0.025$. This indicates that the correlation length is either comparable or much higher than the typical grain size of a polycrystalline materials. Hence, the critical fluctuations is more dominant than the mean-field behaviour in the temperature range $|\epsilon| \leq 0.025$. Our C_P analysis is within this regime of uncertainty hence the non-linear fitting of the $C_P(T \approx T_C)$ yields 3D Ising critical exponents both below and above T_C. The estimation from the magnetization studies is done with temperature interval $|\epsilon| \leq 0.20$ which captures both 3D Ising and the crossover behaviours. Finally, the extended type of interaction can be represented by $J(r) \approx r^{-(d+\sigma)}$, where r is the distance and σ is the range of interaction [16]. For a homogeneous magnet, the susceptibility exponent γ can be expressed by the following relation [32,33]:

$$\gamma = 1 + \frac{4}{d}\left(\frac{n_S+2}{n_S+8}\right)\Delta\sigma + \frac{8(n_S+2)(n_S-4)}{d^2(n_S+8)^2} \times \left(\frac{2G(d/2)(7n_S+20)}{(n_S-4)(n_S+8)}\right)\Delta\sigma^2, \quad (15)$$

where $\Delta\sigma = \sigma - \frac{d}{2}$; $G(d/2) = 3 - \frac{1}{4}(\frac{d}{2})^2$. In the literature, it is customary to solve this equation counterintuitively by choosing a correct set of parameters (d, n_S) in order to find the close γ value for the system. In our case since $d = 3$ and $\gamma \approx 1$, we believe that the trivial solution for eq. (15) would be $\Delta\sigma = 0$ and this leads to $\gamma = 1$. This assumption is not completely unphysical because $\sigma = 1.5$ signifies mean-field behaviour with long-range interaction, whereas $\sigma \approx 2$ implies a short-range ordering [16,30,33]. The critical exponents are inter-connected by the following relations [30]: $\upsilon = \gamma/\sigma$; $\alpha = 2 - \upsilon d$; $\beta = (2 - \alpha - \gamma)/2$; $\delta = 1 + \gamma/\beta$. By using the α and γ values, σ was estimated to be 1.6 which leads to spin interactions $J(r)$ decaying as $r^{-4.587}$ is expected for long-range interactions.

Summary and conclusions. – In conclusion, we observed a large magnetocaloric effect in Gd_2Cu_2In and presented a detailed critical behaviour analysis of the magnetic transition. The isothermal magnetic entropy change (ΔS_m) was observed to be 11.4 J/kg · K and 13.8 J/kg · K for 5 T and 7 T, respectively. The system shows a moderate adiabatic temperature change (ΔT_{ad}) of 6.5 K for 7 T applied field. The PM-FM phase transition is observed to be second order in nature. Four critical exponents (β, γ, δ and α) were estimated using various methods *viz.*, MAP, KF, critical isotherm and non-linear C_P fit. The analysis shows that the exponents belong to 3D Ising behaviour coupled with a long-range interaction. The spontaneous magnetization exponent (β) and heat capacity exponent α values are close to the 3D Ising values, whereas other two exponents indicate a long-range or mean-field–type behaviour. The heat capacity exponent α was estimated using the relation $C_P = B + C\epsilon + A^{\pm}|\epsilon|^{-\alpha}(1 + E^{\pm}|\epsilon|^{0.5})$ in the temperature range $|\epsilon| \leq 0.025$ and the value was observed to be 0.11(2). Finally, the extended range of interaction $J(r)$ decays as $r^{-4.587}$ supports the presence of long-range magnetic ordering.

* * *

RKK acknowledges the FRC/URC Postdoctoral fellowship. AMS thanks the SA-NRF (93549) and the FRC/URC of UJ for financial assistance. RKK thanks Dr. K. R. Prathyusha for critically reading the manuscript.

REFERENCES

[1] Tishin A. M. and Spichkin Y. I., *The Magnetocaloric Effect and its Application* (CRC Press) 2003.
[2] Bruck E., *J. Phys D: Appl. Phys.*, **38** (2005) R381.
[3] Gschneidner K. A. jr., Pecharsky V. and Tsokol A., *Rep. Prog. Phys.*, **68** (2005) 1479.
[4] Singh N. K., Suresh K. G., Nigam A. K., Malik S. K., Coelho A. A. and Gama S., *J. Magn. & Magn. Mater.*, **317** (2007) 68.
[5] Pecharsky V. K. and Gschneidner K. A. jr., *Phys. Rev. Lett.*, **78** (1997) 4494.
[6] Phan M. H. and Yu S. C., *J. Magn. & Magn. Mater.*, **308** (2007) 325.
[7] Fujita A., Fujieda S., Hasegawa Y. and Fukamichi K., *Phys. Rev. B*, **67** (2003) 104416.
[8] Fisher I. R., Islam Z. and Canfield P. C., *J. Magn. & Magn. Mater.*, **202** (1999) 1.
[9] Hulliger F., *J. Alloys Compd.*, **217** (1995) 164.
[10] Zhang Y., Yang Y., Xu X., Geng S., Hou L., Li X. and Wilde G., *Sci. Rep.*, **6** (2016) 34192.
[11] Yi Y., Li L., Su K., Qi Y. and Huo D., *Intermetallics*, **80** (2017) 22.
[12] Yang Y., Zhang Y., Xu X., Geng S., Hou L., Li X. and Wilde G., *J. Alloys Compd.*, **692** (2017) 665.
[13] Zhang Y., Yang Y., Xu X., Hou L., Ren Z., Li X. and Wilde G., *Appl. Phys.*, **49** (2016) 145002.
[14] Li L., Yi Y., Su K., Qi Y., Huo D. and Pöttgen R., *J. Mater. Sci.*, **51** (2016) 5421.
[15] Zhang Y., Xu X., Yang Y., Hou L., Ren Z., Li X. and Wilde G., *J. Alloys Compd.*, **667** (2016) 130.
[16] Li R., Ma Z., Balfour E. A., Fu H. and Luo Y., *J. Alloys Compd.*, **658** (2016) 672.
[17] Li L., Nishimura K., Huo D., Qian Z. and Namiki T., *J. Alloys Compd.*, **572** (2013) 205.
[18] Zheng Z. G., Zhong X. C., Yu H. Y., Franco V., Liu Z. W. and Zeng D. C., *J. Appl. Phys.*, **111** (2012) 07A922.
[19] Kim D., Zink B. L., Hellman F. and Coey J. M. D., *Phys. Rev. B*, **65** (2002) 214424.
[20] Toby B. H., *J. Appl. Crystallogr.*, **34** (2001) 210.
[21] Larson A. C. and Von Dreele R. B., *Gsas, General Structure Analysis System*, LANSCE, MS-H805, Los Alamos, New Mexico.
[22] Kalychak Y., Zaremba V., Baranyak V., Zavalii P., Bruskov V., Sysa L. and Dmytrakh O., *Inorg. Mater.*, **26** (1990) 74.
[23] Oesterreicher H. and Parker F. T., *J. Appl. Phys.*, **55** (1984) 4334.

[24] Franco V., Conde A., Romero-Enrique J. and Blázquez J., *J. Phys.: Condens. Matter*, **20** (2008) 285207.
[25] Bonilla C. M., Bartolomé F., García L. M., Parra-Borderías M., Herrero-Albillos J. and Franco V., *J. Appl. Phys.*, **107** (2010) 09E131.
[26] Fisher M. E., *Rep. Prog. Phys.*, **30** (1967) 615.
[27] Franco V., Blázquez J. S. and Conde A., *Appl. Phys. Lett.*, **89** (2006) 222512.
[28] Oleaga A., Salazar A., Thamizhavel A. and Dhar S. K., *J. Alloys Compd.*, **617** (2014) 534.
[29] Oleaga A. A., Salazar M., Ciomaga Hatnean and Geetha Balakrishnan, *Phys. Rev. B*, **92** (2015) 024409.
[30] Liu B., Zou Y., Zhang L., Zhou S., Wang Z., Wang W., Qu Z. and Zhang Y., *Sci. Rep.*, **6** (2016) 33873.
[31] Dey K., Indra A., Majumdar S. and Giri S., *J. Magn. & Magn. Mater.*, **435** (2017) 15.
[32] Fisher M. E., *Rev. Mod. Phys.*, **46** (1974) 597.
[33] Nair S., Banerjee A., Narlikar A. V., Prabhakaran D. and Boothroyd A. T., *Phys. Rev. B*, **68** (2003) 132404.